

# Combined Convective Boundary Layer Flow Over a Horizontal Plate Embedded in a Porous Medium Saturated with a Nanofluid

Mahesh Kumari<sup>1</sup> and Rama Subba Reddy Gorla<sup>2</sup>

<sup>1</sup>Department of Mathematics, Indian Institute of Science, Bangalore - 560012, India

Email: mkumari@math.iisc.ernet.in

<sup>2</sup>Cleveland State University, Cleveland, Ohio 44115 USA

Email: r.gorla@csuohio.edu

## ABSTRACT

A boundary layer analysis is presented for the mixed convection past a horizontal plate in a porous medium saturated with a nano fluid. The prescribed heat and mass flux boundary conditions are considered. The entire regime of the mixed convection is included, as the mixed convection parameter  $\xi$  varies from 0 (pure free convection) to 1 (pure forced convection). The transformed nonlinear system of equations is solved by using an implicit infinite difference method. Numerical results for friction factor, surface heat transfer rate and mass transfer rate have been presented for parametric variations of the buoyancy ratio parameter  $N_r$ , Brownian motion parameter  $N_b$ , thermophoresis parameter  $N_t$  and Lewis number  $Le$ . The dependency of the friction factor, surface heat transfer rate (Nusselt number) and mass transfer rate on these parameters has been discussed.

**Keywords:** mixed convection, porous medium, nanofluid

## NOMENCLATURE

$D_B$	Brownian diffusion coefficient
$D_T$	thermophoretic diffusion coefficient
$f$	rescaled nano-particle volume fraction
$g$	gravitational acceleration vector
$k_m$	effective thermal conductivity of the porous medium
$K$	permeability of porous medium
$Le$	Lewis number
$N_r$	Buoyancy Ratio
$N_b$	Brownian motion parameter
$N_t$	thermophoresis parameter
$Nu$	Nusselt number
$P$	pressure
$q''$	wall heat flux
$Ra_x$	local Rayleigh number
$Re$	Reynolds number
$S$	dimensionless stream function
$T$	temperature
$T_w$	wall temperature of the plate

---

\*Corresponding author: r.gorla@csuohio.edu

$T_\infty$	ambient temperature
$U$	reference velocity
$u, v$	Darcy velocity components
$(x, y)$	Cartesian coordinates

**Greek Symbols:**

$\alpha_m$	thermal diffusivity of porous medium
$\beta$	volumetric expansion coefficient of fluid
$\varepsilon$	porosity
$\eta$	dimensionless distance
$\theta$	dimensionless temperature
$\mu$	viscosity of fluid
$\rho_f$	fluid density
$\rho_p$	nano-particle mass density
$(\rho c)_f$	heat capacity of the fluid
$(\rho c)_m$	effective heat capacity of porous medium
$(\rho c)_p$	effective heat capacity of nano-particle material
$\tau$	parameter defined by equation (13)
$\phi$	nano-particle volume fraction
$\phi_w$	nano-particle volume fraction at the wall of the plate
$\phi_\infty$	ambient nano-particle volume fraction
$\Psi$	stream function

**1. INTRODUCTION**

Recently, there has been a lot of interest in the study of augmenting convective heat transfer in engineering applications. Low thermal conductivity of conventional heat transfer fluids such as water, oil, and ethylene glycol is a serious limitation in improving the performance and compactness of heat exchangers and electronic devices. The thermal conductivities of fluids with dispersed particles are expected to be higher than that of conventional fluids. Nanofluids are new heat transfer fluids containing a small quantity of nano-sized particles (usually less than 100 nm) that are uniformly and stably dispersed in a liquid. The dispersion of a small amount of solid nanoparticles in conventional fluids changes their thermal conductivity remarkably. Compared to the existing techniques for enhancing heat transfer, the nanofluids show a superior potential for increasing heat transfer rates in a variety of cases. The nanofluids have many applications in the industry and have unique physical and chemical properties. A small amount (< 1% volume fraction) of Cu nanoparticles or carbon nanotubes dispersed in ethylene glycol or oil is reported to increase the inherently poor thermal conductivity of the liquid by 40% and 150%, respectively as reported by Eastman et al. [1] and Choi et al. [2]. Conventional particle-liquid suspensions require high concentrations (> 10%) of particles to achieve such enhancement. However, problems of rheology and stability are amplified at high concentrations, precluding the widespread use of conventional slurries as heat transfer fluids. In some cases, the observed enhancement in thermal conductivity of nanofluids is orders of magnitude larger than predicted by well-established theories. Other perplexing results in this rapidly evolving field include a surprisingly strong temperature dependence of the thermal conductivity as reported by Patel et al. [3] and a three-fold higher critical heat flux compared with the base fluids as reported by You et al. [4] and Vassallo et al. [5]. These enhanced thermal properties are not merely of academic interest. If confirmed and found consistent, they would make nanofluids promising for applications in thermal management. Furthermore, suspensions of metal nanoparticles are also being developed for other purposes, such as medical applications including cancer therapy. The interdisciplinary nature of nanofluid research presents a great opportunity for exploration and discovery at the frontiers of nanotechnology.

Nanofluids may be prepared either by a single- or two-step process. In the two-step process the nanoparticles are separately synthesized and then dispersed in the base fluid, while in the single-step

process the synthesis of nanoparticles is combined with the preparation of nanofluids, as the nanoparticles synthesized (say, by physical/chemical vapor deposition or wet chemical methods) are collected (stabilized) in the same fluid/medium.

Porous media heat transfer problems have several engineering applications such as geothermal energy recovery, crude oil extraction, ground water pollution, thermal energy storage and flow through filtering media. Cheng and Minkowycz [6] presented similarity solutions for free convective heat transfer from a vertical plate in a fluid-saturated porous medium. Gorla and co-workers [7, 8] solved the nonsimilar problem of free convective heat transfer from a vertical plate embedded in a saturated porous medium with an arbitrarily varying surface temperature or heat flux. Chen and Chen [9] and Mehta and Rao [10] presented similarity solutions for free convection of non-Newtonian fluids over horizontal surfaces in porous media. Nakayama and Koyama [11] studied the mixed convection over a non-isothermal body of arbitrary geometry placed in a porous medium. All these studies were concerned with Newtonian fluid flows. The boundary layer flows in nano fluids have been analyzed recently by Nield and Kuznetsov [12] and Nield and Kuznetsov [13]. A clear picture about the nanofluid boundary layer flows is still to emerge.

The present work has been undertaken in order to analyze the mixed convection past an isothermal horizontal plate in a porous medium saturated by a nanofluid. The effects of Brownian motion and thermophoresis are included for the nanofluid. Numerical solutions of the boundary layer equations are obtained and discussion is provided for several values of the nanofluid parameters governing the problem.

**2. ANALYSIS**

We consider the steady mixed convection boundary layer flow past a horizontal plate placed in a nano-fluid saturated porous medium. The co-ordinate system is selected such that x-axis is in the horizontal direction. We consider the two-dimensional problem. Figure 1 shows the coordinate system and flow model. At the surface, the temperature  $T$  and the nano-particle fraction  $\phi$  take constant values  $T_w$  and  $\phi_w$ , respectively. The ambient values, attained as  $y$  tends to infinity, of  $T$  and  $\phi$  are denoted by  $T_\infty$  and  $\phi_\infty$ , respectively.

The Oberbeck-Boussinesq approximation is employed and the homogeneity and local thermal equilibrium in the porous medium are assumed. We consider the porous medium whose porosity is denoted by  $\varepsilon$  and permeability by  $K$ . The Darcy velocity is denoted by  $\vec{v}$ . The following four field equations embody the conservation of total mass, momentum, thermal energy, and nano-particles, respectively. The field variables are the Darcy velocity  $\vec{v}$ , the temperature  $T$  and the nano-particle volume fraction  $\phi$ .

$$\nabla \cdot \vec{v} = 0 \tag{1}$$

$$\frac{\rho_f}{\varepsilon} \frac{\partial \vec{v}}{\partial t} = -\nabla P - \frac{\mu}{K} \vec{v} + \left[ \phi \rho_p + (1 - \phi) \left\{ \rho_f (1 - \beta (T - T_\infty)) \right\} \right] \vec{g} \tag{2}$$

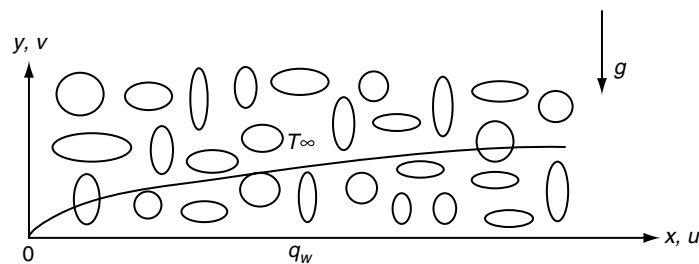


Figure 1. Coordinate system and flow model.

$$(\rho c)_m \frac{\partial T}{\partial t} + (\rho c)_f \vec{v} \cdot \nabla T = k_m \nabla^2 T + \varepsilon (\rho c)_p \left[ D_B \nabla \phi \cdot \nabla T + \frac{D_T}{T_\infty} \nabla T \cdot \nabla T \right] \quad (3)$$

$$\frac{\partial \phi}{\partial t} + \frac{1}{\varepsilon} \vec{v} \cdot \nabla \phi = D_B \nabla^2 \phi + \frac{D_T}{T_\infty} \nabla^2 T \quad (4)$$

We write  $\vec{v} = (u, v)$ .

Here  $\rho_f, \mu$  and  $\beta$  are the density, viscosity and volumetric volume expansion coefficient of the fluid;  $\rho_p$  the density of the particles;  $g$  the gravitational acceleration;  $(\rho c)_m$  the effective heat capacity and  $k_m$  effective thermal conductivity of the porous medium and  $D_B$  the Brownian diffusion coefficient and  $D_T$  the thermophoretic diffusion coefficient. The flow is assumed to be slow so that an advective term and a Forchheimer quadratic drag term do not appear in the momentum equation.

The boundary conditions are taken to be

$$v = 0, \quad \frac{\partial T}{\partial y} = -\frac{q_w}{k_f}, \quad \frac{\partial \phi}{\partial y} = -\frac{m_w}{D_B} \quad \text{at } y = 0 \quad (5)$$

$$u = 0, \quad T \rightarrow T_\infty, \quad \phi \rightarrow \phi_\infty, \quad \text{as } y \rightarrow \infty \quad (6)$$

The wall temperature and concentration are assumed as:

$$q_w = a x^n \quad \text{and} \quad m_w = b x^n.$$

We consider the steady state flow. In keeping with the Oberbeck-Boussinesq approximation and an assumption that the nano-particle concentration is dilute, the momentum equation may be written as:

$$0 = -\nabla P - \frac{\mu}{K} \vec{v} + \left[ (\rho_p - \rho_{f\infty})(\phi - \phi_\infty) + (1 - \phi_\infty) \rho_{f\infty} \beta (T - T_\infty) \right] \vec{g} \quad (7)$$

We now make the standard boundary layer approximation based on a scale analysis and write the governing equations.

$$\frac{\partial u}{\partial x} + \frac{\partial v}{\partial y} = 0 \quad (8)$$

$$\frac{\partial P}{\partial x} = -\frac{\mu}{K} u \quad (9)$$

$$\frac{\partial P}{\partial y} = \left[ (1 - \phi_\infty) \rho_{f\infty} \beta g (T - T_\infty) - (\rho_p - \rho_{f\infty}) g (\phi - \phi_\infty) \right] \quad (10)$$

$$u \frac{\partial T}{\partial x} + v \frac{\partial T}{\partial y} = \alpha_m \frac{\partial^2 T}{\partial y^2} + \tau \left[ D_B \frac{\partial \phi}{\partial y} \frac{\partial T}{\partial y} + \left( \frac{D_T}{T_\infty} \right) \left( \frac{\partial T}{\partial y} \right)^2 \right] \quad (11)$$

$$\frac{1}{\varepsilon} \left( u \frac{\partial \phi}{\partial x} + v \frac{\partial \phi}{\partial y} \right) = D_B \frac{\partial^2 \phi}{\partial y^2} + \left( \frac{D_T}{T_\infty} \right) \frac{\partial^2 T}{\partial y^2} \tag{12}$$

where

$$\alpha_m = \frac{k_m}{(\rho c)_f}, \quad \tau = \frac{\varepsilon(\rho c)_p}{(\rho c)_f} \tag{13}$$

One can eliminate  $P$  from equations (9) and (10) by cross-differentiation. At the same time one can introduce a stream line function  $\psi$  such that the continuity is automatically satisfied:

$$u = \frac{\partial \psi}{\partial y}, \quad v = -\frac{\partial \psi}{\partial x} \tag{14}$$

We are then left with the following three equations.

$$\frac{\partial^2 \psi}{\partial y^2} = -\frac{(1 - \phi_\infty) \rho_{f\infty} \beta g K}{\mu} \frac{\partial T}{\partial x} + \frac{(\rho_p - \rho_{f\infty}) g K}{\mu} \frac{\partial \phi}{\partial x} \tag{15}$$

$$\frac{\partial \psi}{\partial y} \frac{\partial T}{\partial x} - \frac{\partial \psi}{\partial x} \frac{\partial T}{\partial y} = \alpha_m \nabla^2 T + \tau \left[ D_B \frac{\partial \phi}{\partial y} \frac{\partial T}{\partial y} + \left( \frac{D_T}{T_\infty} \right) \left( \frac{\partial T}{\partial y} \right)^2 \right] \tag{16}$$

$$\frac{1}{\varepsilon} \left( \frac{\partial \psi}{\partial y} \frac{\partial \phi}{\partial x} - \frac{\partial \psi}{\partial x} \frac{\partial \phi}{\partial y} \right) = D_B \frac{\partial^2 \phi}{\partial y^2} + \left( \frac{D_T}{T_\infty} \right) \frac{\partial^2 T}{\partial y^2} \tag{17}$$

Proceeding with the analysis we introduce the following dimensionless variables:

$$\eta = \frac{y}{x} \cdot Pe_x^{1/2} \xi^{-1}$$

$$\xi = 1 / \left[ 1 + (Ra_x / Pe_x^2)^{1/4} \right]$$

$$Ra_x = \frac{(1 - \phi_\infty) \rho_{f\infty} \beta g K x}{\mu \cdot \alpha_m} \left( \frac{q_w x}{k_m} \right)$$

$$Pe_x = \frac{u_\infty x}{\alpha_m}$$

$$\begin{aligned}
 S &= \frac{\psi \xi}{\alpha_m \cdot Pe_x^{1/2}} \\
 \theta &= \frac{T - T_\infty}{\left(\frac{q_w x}{k_m}\right) \xi Pe_x^{-1/2}} \\
 f &= \frac{\phi - \phi_\infty}{\left(\frac{m_w x}{D_B}\right) \xi Pe_x^{-1/2}}
 \end{aligned}
 \tag{18}$$

Substituting the expressions in equation (18) into the governing equations (15)–(17) we obtain the following transformed equations:

$$\begin{aligned}
 S'' + (1-\xi)^4 \cdot \left[ \frac{2n+1}{2} - (1-\xi) \left( \frac{n}{4} \right) \right] (\theta - N_r f) + (1-\xi)^4 \cdot \left[ -\frac{1}{2} + (1-\xi) \left( \frac{n}{4} \right) \right] \cdot \eta \cdot (\theta' - N_r f') \\
 = \xi (1-\xi)^5 \cdot \left( \frac{n}{4} \right) \left( \frac{\partial \theta}{\partial \xi} - N_r \frac{\partial f}{\partial \xi} \right)
 \end{aligned}
 \tag{19}$$

$$\begin{aligned}
 \theta'' + \left[ \frac{1}{2} + (1-\xi) \left( \frac{n}{4} \right) \right] \cdot S \theta' - \left[ \frac{2n+1}{2} - (1-\xi) \left( \frac{n}{4} \right) \right] S' \theta + N_b \cdot f' \cdot \theta' + N_t (\theta')^2 \\
 = -\frac{n\xi(1-\xi)}{4} \left[ S' \frac{\partial \theta}{\partial \xi} - \theta' \frac{\partial S}{\partial \xi} \right]
 \end{aligned}
 \tag{20}$$

$$\begin{aligned}
 \frac{1}{Le} f'' + \frac{1}{Le} \frac{N_t}{N_b} \theta'' + \left[ \frac{1}{2} + (1-\xi) \left( \frac{n}{4} \right) \right] \cdot S f' - \left[ \frac{2n+1}{2} - (1-\xi) \left( \frac{n}{4} \right) \right] S' f \\
 = -\frac{n\xi(1-\xi)}{4} \left[ S' \frac{\partial f}{\partial \xi} - f' \frac{\partial S}{\partial \xi} \right]
 \end{aligned}
 \tag{21}$$

where the parameters are defined as:

$$N_r = \frac{(\rho_P - \rho_{f\infty}) m_w k_m}{\rho_{f\infty} \beta (1 - \phi_\infty) q_w D_B},$$

$$N_b = \frac{\varepsilon (\rho c)_P D_B (\phi_w - \phi_\infty)}{(\rho c)_f \alpha_m},$$

$$N_t = \frac{\varepsilon (\rho c)_P D_T (T_w - T_\infty)}{(\rho c)_f \alpha_m T_\infty},$$

$$Le = \frac{\alpha_m}{\varepsilon \cdot D_B},$$

$$Re_x = \frac{u_\infty x}{\nu} \tag{22}$$

The transformed boundary conditions are:

$$\eta = 0: \quad S = 0, \quad \theta' = -1, \quad f' = -1$$

$$\eta \rightarrow \infty: \quad S' = \xi^2, \quad \theta = 0, \quad f = 0 \tag{23}$$

The local friction factor may be written as

$$C_{fx} = \frac{\left(\mu \frac{\partial u}{\partial y}\right)_{y=0}}{\frac{\rho U_\infty^2}{2}} = \frac{2 \left[ Pe_x^{\frac{1}{2}} + Ra_x^{\frac{1}{4}} \right]^3}{Re_x Pe_x} S''(\xi, 0) \tag{24}$$

The heat transfer rate at the surface is given by:

$$q_W = -k_m \left. \frac{\partial T}{\partial y} \right)_{y=0}$$

The heat transfer coefficient is given by:

$$h = \frac{q_W}{(T_W - T_\infty)}$$

Local Nusselt number is given by:

$$Nu_x = \frac{h \cdot x}{k_m} = \left[ Pe_x^{1/2} + Ra_x^{1/4} \right] / \theta(\xi, 0) \tag{25}$$

The mass transfer rate at the surface is given by:

$$m_W = -D_B \left. \frac{\partial \phi}{\partial y} \right)_{y=0}, \quad h_m = \frac{m_W}{(\phi_W - \phi_\infty)}$$

where  $h_m$  = mass transfer coefficient,

The local Sherwood number is given by:

$$Sh = \frac{h_m \cdot x}{D_B} = \left[ Pe_x^{1/2} + Ra_x^{1/4} \right] / f(\xi, 0) \tag{26}$$

### 3. NUMERICAL METHOD

The system of equations (19)–(21) with the boundary conditions (23) is solved numerically by means of an efficient, iterative, tri-diagonal implicit finite-difference method discussed previously by Blottner [14]. Equations (19)–(21) are discretized using three-point central difference formulae with  $S'$  replaced by another variable  $V$ . The  $\eta$  direction is divided into 196 nodal points and a variable step size is used to account for the sharp changes in the variables in the region close to the surface where viscous effects dominate. The initial step size used is  $\Delta\eta_1 = 0.001$  and the growth factor  $K = 1.037$  such that  $\Delta\eta_n = K\Delta\eta_{n-1}$  (where the subscript  $n$  is the number of nodes minus one). This gives  $\eta_{\max} \approx 35$  which represents the edge of the boundary layer at infinity. The ordinary differential equations are then converted into linear algebraic equations that are solved by the Thomas algorithm discussed by Blottner [14]. Iteration is employed to deal with the nonlinear nature of the governing equations. The convergence criterion employed in this work was based on the relative difference between the current and the previous iterations. When this difference or error reached  $10^{-5}$ , the solution was assumed converged and the iteration process was terminated.

### 4. RESULTS AND DISCUSSION

Equations (19–21) were solved numerically to satisfy the boundary conditions (23) for parametric values of  $Le$ ,  $N_r$  (buoyancy ratio number),  $N_b$  (Brownian motion parameter) and  $N_t$  (thermophoresis parameter) using finite difference method. Figure 2 shows a comparison of our results with literature data reported by Aldoss et al. [16] for the Newtonian fluid case. A comparison of our results with literature data suggests that the present results are highly accurate.

Figure 3 shows that  $N_r$  does not have appreciable influence on the velocity, temperature and concentration profiles. The parameter  $N_r$  appears only in the momentum boundary layer equation. Buoyancy is principally a macroscale effect. The buoyancy influences the velocity and temperature fields, however, has a minor effect on nano particle diffusion. This explains the minor influence of buoyancy on the profiles.

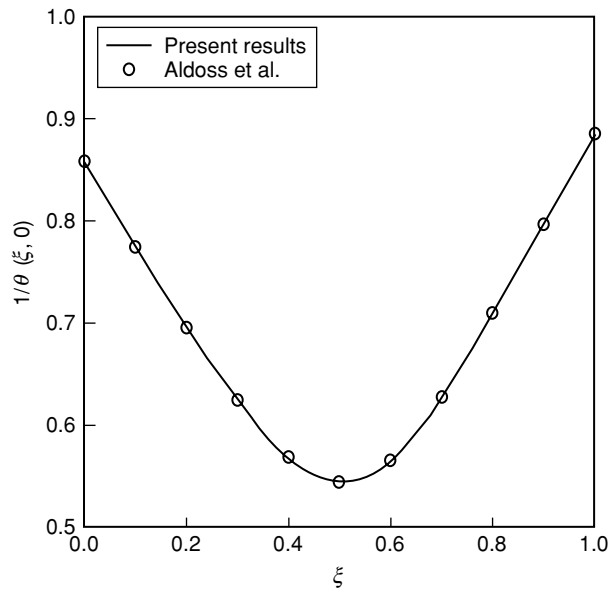


Figure 2. Comparison of heat transfer results for  $N_r=0$ ,  $N_t=0$ ,  $N_b=0$ ,  $n=0.0$ .

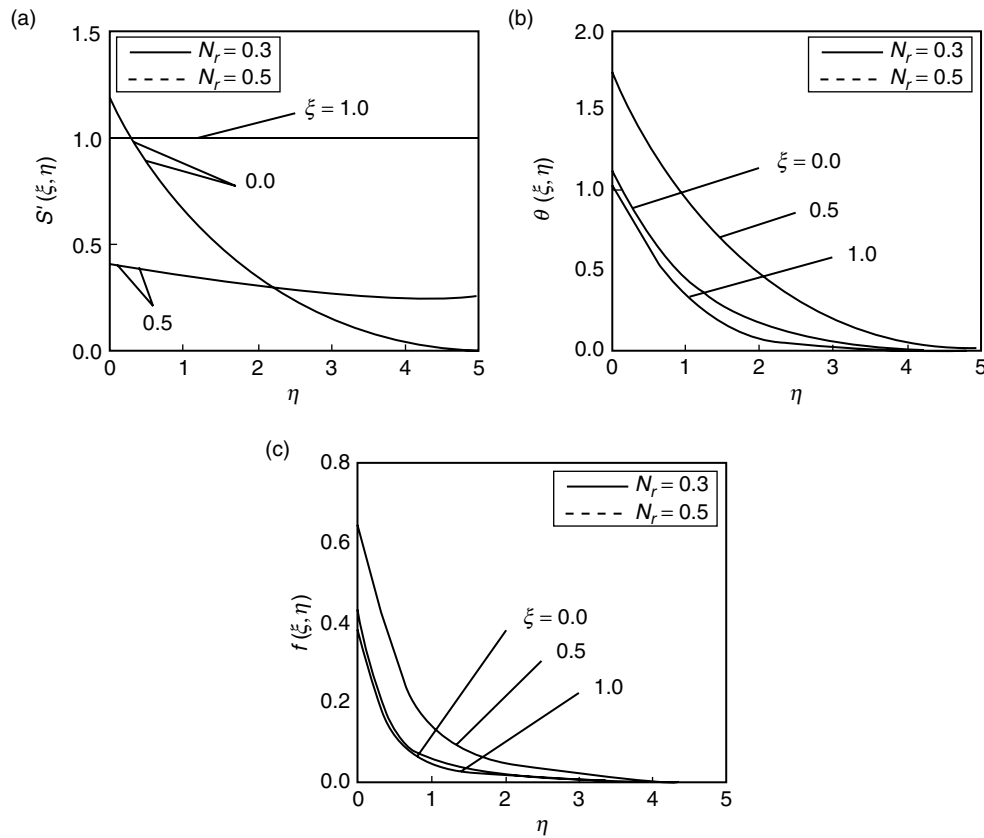


Figure 3. Effects of  $N_r$  and  $\xi$  on velocity, temperature and concentration profiles for  $N_t=0.01$ ,  $N_b=0.01$ ,  $n=0.1$  and  $Le=10$ .

Similar effects are observed from Figures 4 and 5 as  $N_t$  and  $N_b$  vary. Thermophoresis parameter,  $N_t$  appears in the thermal and concentration boundary layer equations. As we note, it is coupled with temperature function and plays a strong role in determining the diffusion of heat and nanoparticle concentration in the boundary layer. From Figure 4, we note that the temperature and nanoparticle concentration increase as  $N_t$  increases whereas the velocity decreases with increasing values of  $N_t$ .  $N_b$  is the Brownian motion parameter. Brownian motion decelerates the flow in the nanofluid boundary layer. Brownian diffusion promotes heat conduction. The nanoparticles increase the surface area for heat transfer. Nanofluid is a two phase fluid where the nanoparticles move randomly and increase the energy exchange rates. Brownian motion reduces nanoparticle diffusion. From Figure 5, we note that velocity, temperature and concentration increase with increasing values of  $N_b$ .

Figure 6 show that as  $Le$  increases, the temperature and concentration within the boundary layer decrease and the thermal and concentration boundary layer thicknesses decrease. The velocity increases as  $Le$  increases.  $Le$  represents the ratio of molecular thermal diffusivity to mass diffusivity ( $Sh$  and  $Pr$ ). As  $Le$  increases, the thermal diffusivity is more pronounced than the mass diffusivity. Since large values of  $Le$  make the molecular diffusivity smaller, concentration decreases as  $Le$  increases.

Figure 7 shows that as the power law exponent for wall temperature/concentration  $n$  increases, the velocity, temperature and concentration decrease.

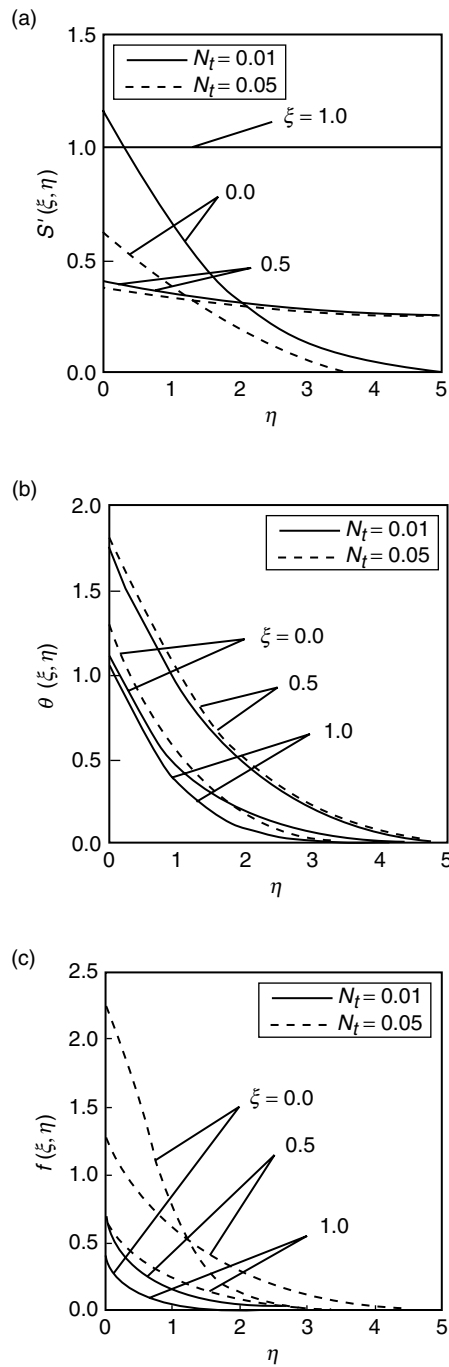


Figure 4. Effects of  $N_t$  and  $\xi$  on velocity, temperature and concentration profiles for  $N_r=0.5$ ,  $N_b=0.01$ ,  $n=0.1$  and  $Le=10$ .

Figures 8–12 display results for wall values for the gradients of velocity, temperature and concentration functions which are proportional to the friction factor, Nusselt number and Sherwood number, respectively. From Figure 8, we notice that as  $N_r$  increases, the friction factor, heat transfer rate (Nusselt number) and mass transfer rate (Sherwood number) decrease. Figure 9 shows that as  $N_t$  increases, the heat and mass

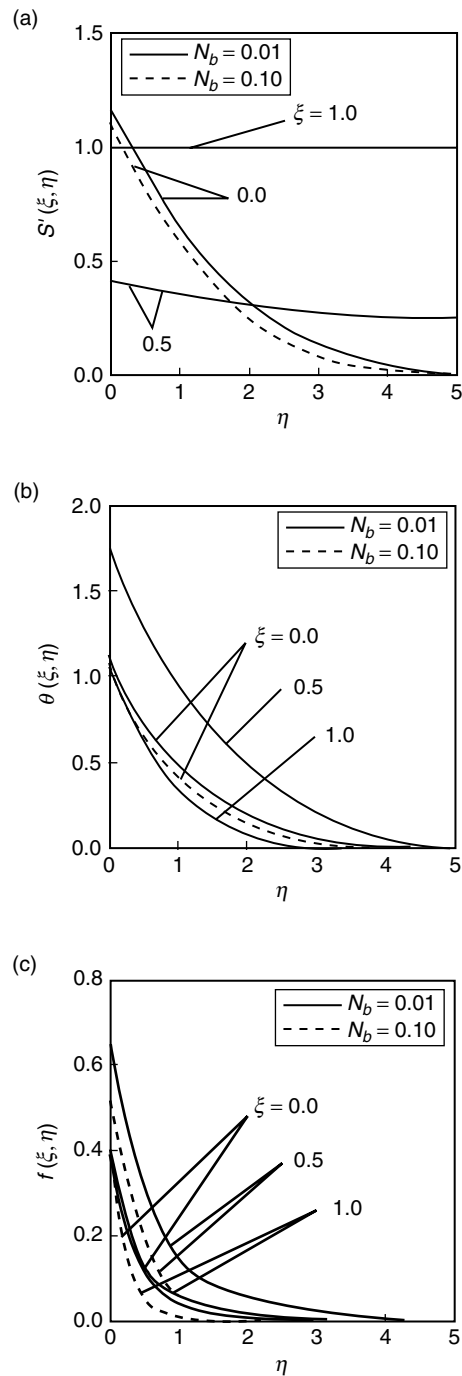


Figure 5. Effects of  $N_b$  and  $\xi$  on velocity, temperature and concentration profiles for  $N_r=0.5$ ,  $N_t=0.01$ ,  $n=0.1$  and  $Le=10$ .

transfer rates decrease. As  $N_b$  increases, the surface mass transfer rates increase whereas the surface heat transfer rate decreases as shown by Figure 10. Figure 11 indicates that as  $Le$  increases, the friction factor as well as the heat and mass transfer rates increase. From Figure 12, we observe that as the power law exponent for wall temperature/concentration  $n$  increases, the heat and mass transfer rates increase.

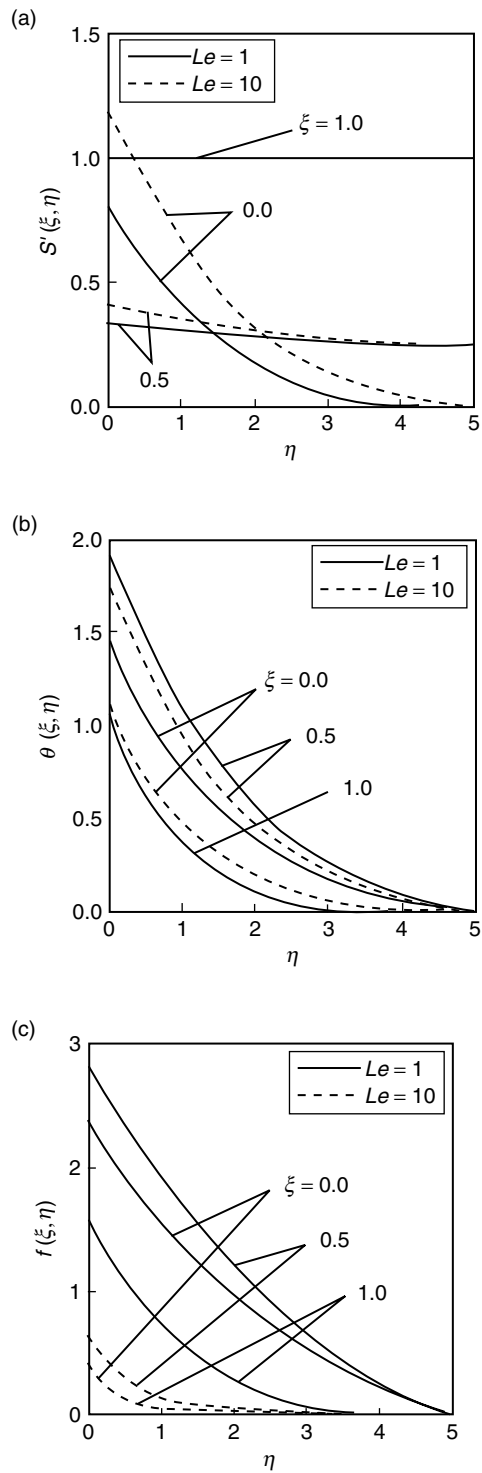


Figure 6. Effects of  $Le$  and  $\xi$  on velocity, temperature and concentration profiles for  $N_r=0.3$ ,  $N_t=0.01$ ,  $N_b=0.01$  and  $n=0.1$ .

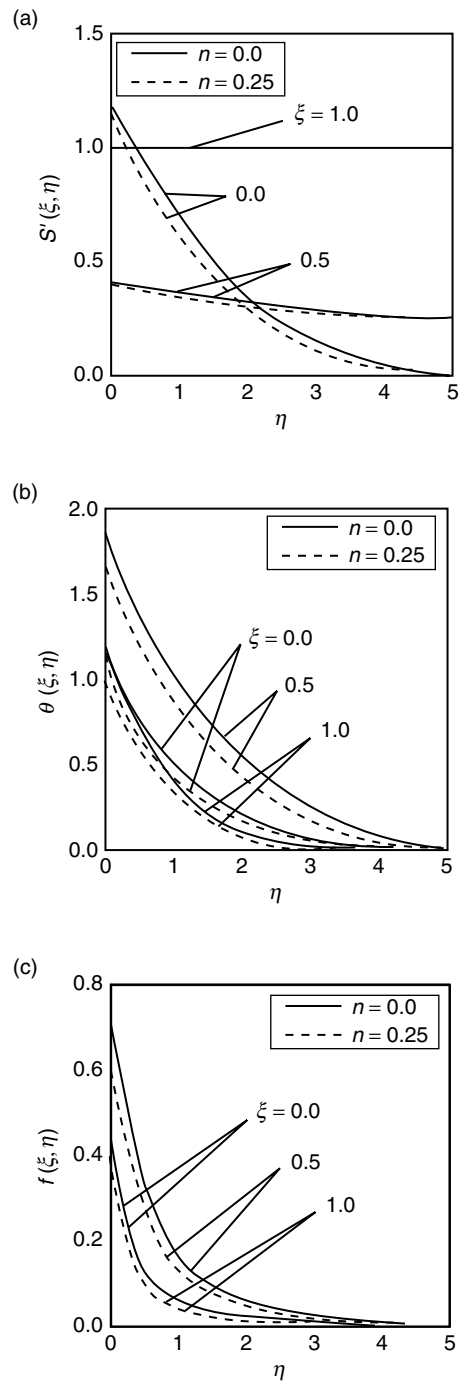


Figure 7. Effects of  $n$  and  $\xi$  on velocity, temperature and concentration profiles for  $N_r=0.5$ ,  $N_t=0.01$ ,  $N_b=0.01$  and  $Le=10$ .

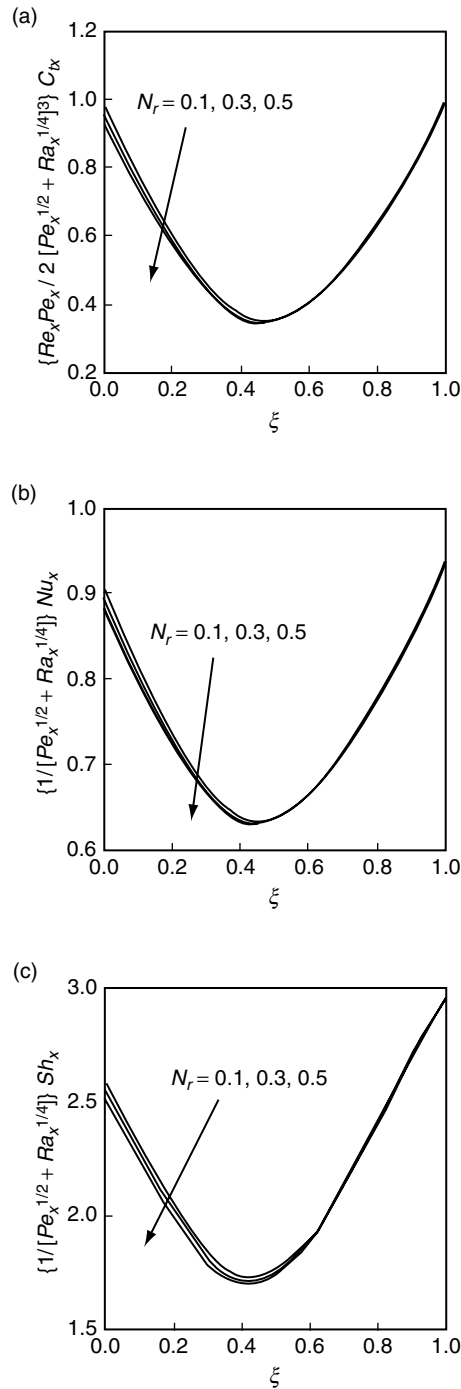


Figure 8. Effects of  $N_r$  and  $\xi$  on skin friction, Nusselt and Sherwood numbers for  $N_t=0.1$ ,  $N_b=0.3$ ,  $n=0.25$  and  $Le=10$ .

The influence of nanoparticles on mixed convection is modeled by accounting for Brownian motion and thermophoresis as well as non-isothermal boundary conditions. The thickness of the boundary layer for the mass fraction is smaller than the thermal boundary layer thickness for large values of Lewis number,  $Le$ . The contribution of  $N_t$  to heat and mass transfer does not depend on the value of  $Le$ . The

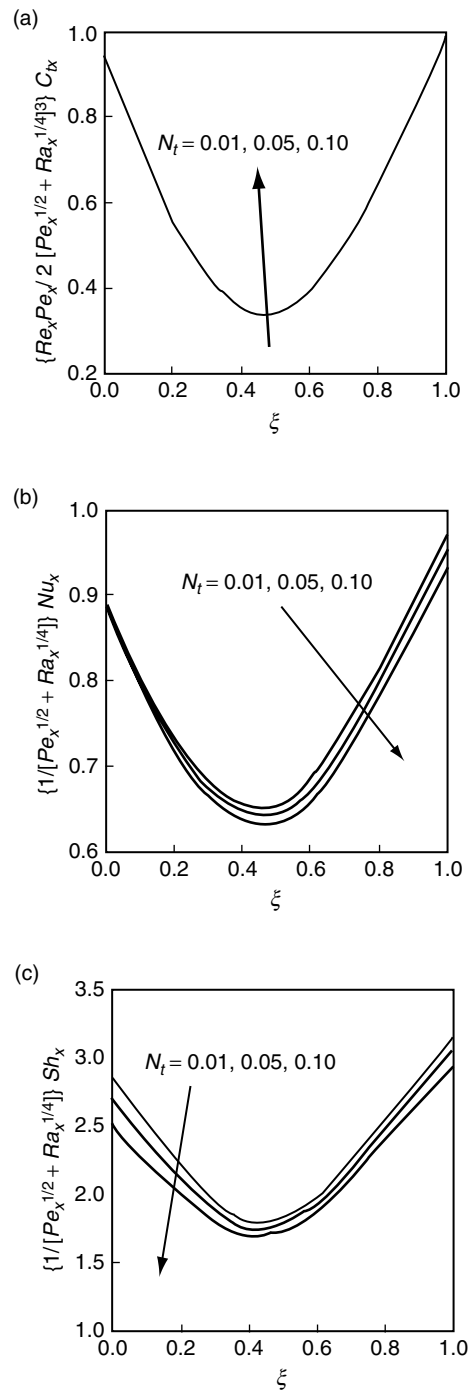


Figure 9. Effects of  $N_t$  and  $\xi$  on skin friction, Nusselt and Sherwood numbers for  $N_r=0.5$ ,  $N_b=0.3$ ,  $n=0.25$  and  $Le=10$ .

Brownian motion and thermophoresis of nano particles increases the effective thermal conductivity of the nanofluid. Both Brownian diffusion and thermophoresis give rise to cross diffusion terms that are similar to the familiar Soret and Dufour cross diffusion terms that arise with a binary fluid discussed by Lakshmi Narayana et al. [17].

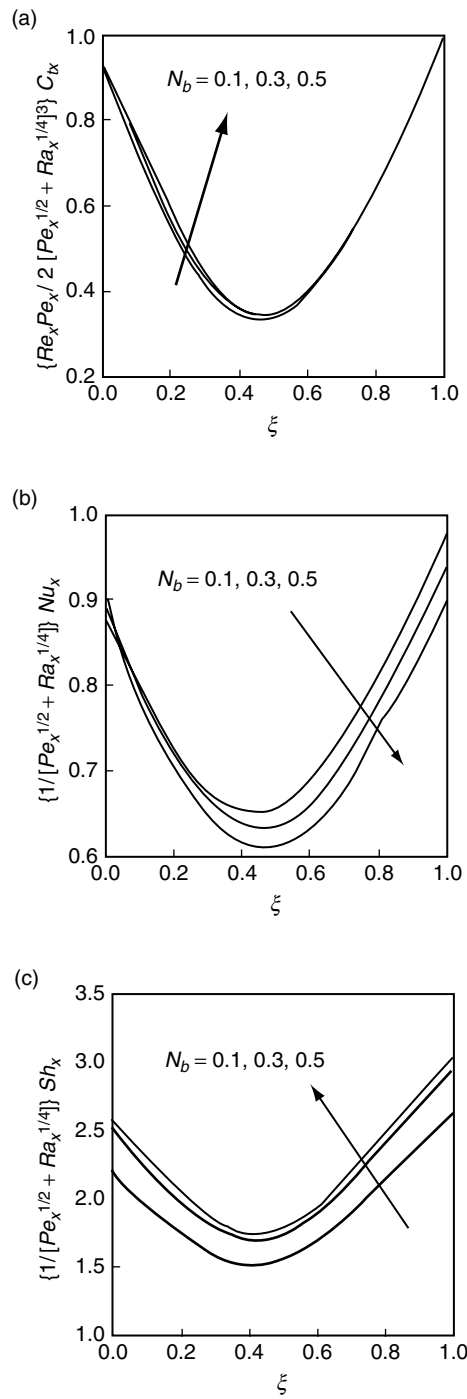


Figure 10. Effects of  $N_b$  and  $\xi$  on skin friction, Nusselt and Sherwood numbers for  $N_r=0.5$ ,  $N_t=0.1$ ,  $n=0.25$  and  $Le=10$ .

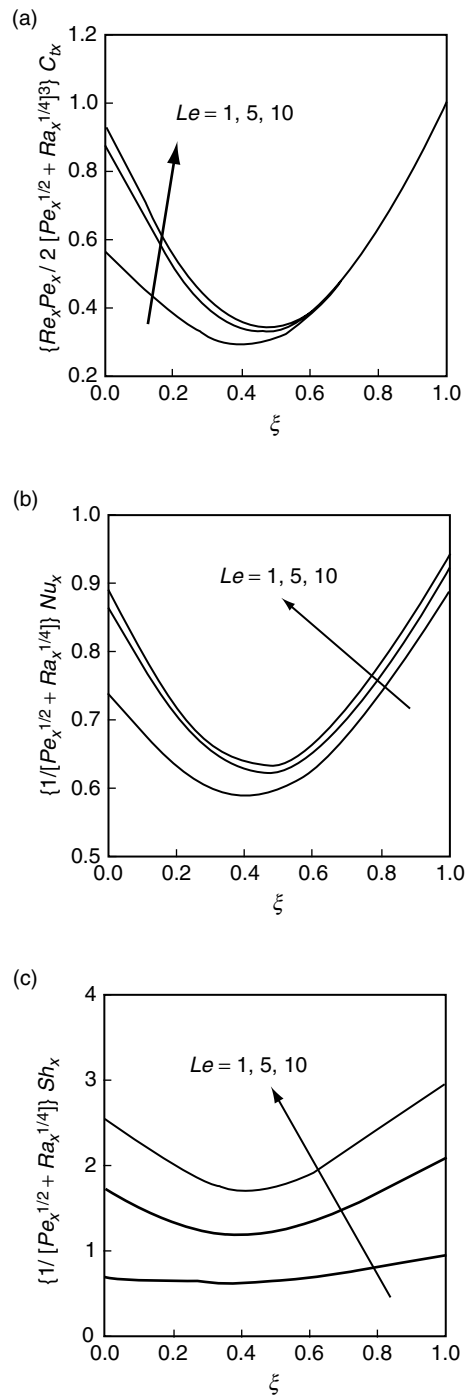


Figure 11. Effects of  $Le$  and  $\xi$  on skin friction, Nusselt and Sherwood numbers for  $N_r=0.5$ ,  $N_t=0.1$ ,  $N_b=0.3$  and  $n=0.25$ .

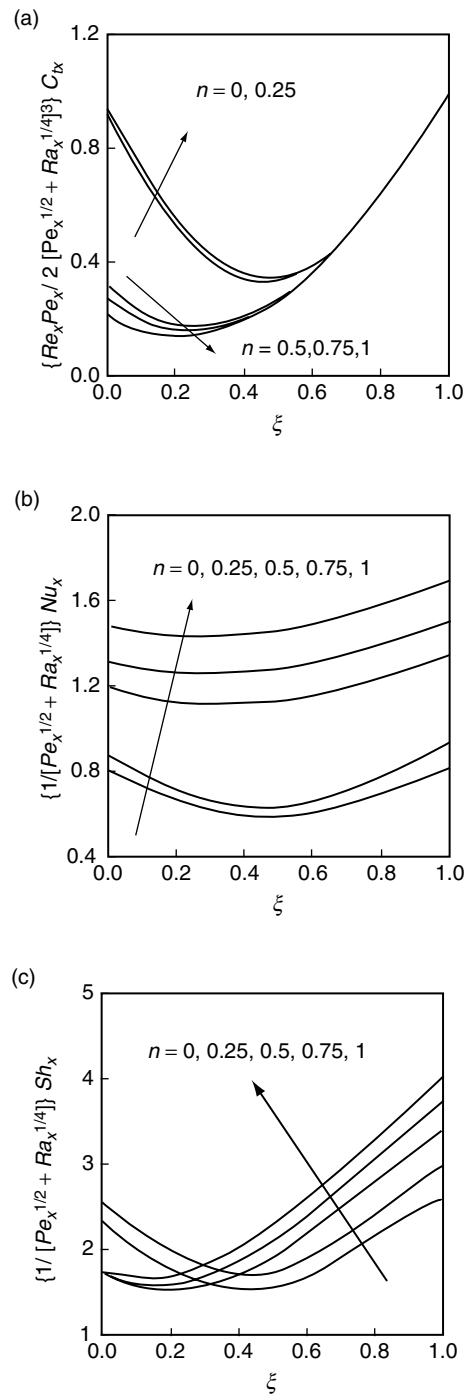


Figure 12. Effects of  $n$  and  $\xi$  on skin friction, Nusselt and Sherwood numbers for  $N_r=0.5$ ,  $N_t=0.1$ ,  $N_b=0.3$  and  $Le=10$ .

### 5. CONCLUDING REMARKS

In this paper, we presented a boundary layer analysis for the mixed convection past a non-isothermal horizontal plate in a porous medium saturated with a nano fluid. Numerical results for friction factor, surface heat transfer rate and mass transfer rate have been presented for parametric variations of the

buoyancy ratio parameter  $N_r$ , Brownian motion parameter  $N_b$ , thermophoresis parameter  $N_t$  and Lewis number  $Le$ . The results indicate that as  $N_r$  and  $N_t$  increase, the heat transfer rate (Nusselt number) and mass transfer rate (Sherwood number) decrease. As  $N_b$  increases, the friction factor and surface mass transfer rates increase whereas the surface heat transfer rate decreases. As  $Le$  increases, the heat and mass transfer rates increase.

#### ACKNOWLEDGEMENT

One of the authors (MK) is thankful to the University Grants Commission, India, for the financial support under the Research Scientist Scheme.

#### REFERENCES

- [1] Eastman, J.A., Choi, S.U.S., Li, S., Yu, W. and Thompson, L.J.: Anomalous Increased Effective Thermal Conductivities Containing Copper Nanoparticles, *Applied Physics Letters*, 78, 718–720 (2001).
- [2] Choi, S.U.S., Zhang, Z.G., Yu, W., Lockwood, F.E. and Grulke, E.A.: Anomalous Thermal Conductivity Enhancement on Nanotube Suspensions, *Applied Physics Letters*, 79, 2252–2254 (2001).
- [3] Patel, H.E., Das, S.K., Sundararajan, T., Sreekumaran, A., George, B. and Pradeep, T: Thermal Conductivities of Naked and Monolayer Protected Metal Nanoparticle Based Nanofluids: Manifestation of Anomalous Enhancement and Chemical Effects, *Applied Physics Letters*, 83, 2931–2933 (2003).
- [4] You, S.M., Kim, J.H. and Kim, K.H.: Effect of Nanoparticles on Critical Heat Flux of Water in Pool Boiling Heat Transfer, *Applied Physics Letters*, 83, 3374–3376 (2003).
- [5] Vassallo, P., Kumar, R. and D'Amico, S.: Pool Boiling Heat Transfer Experiments in Silica-Water Nanofluids, *International Journal of Heat and Mass Transfer*, 47, 407–411 (2004).
- [6] Cheng, P. and Minkowycz, W.J.: Free Convection about a vertical flat plate embedded in a saturated porous medium with applications to heat transfer from a dike, *J. Geophysics. Res.*, 82, 2040–2044 (1977).
- [7] Gorla, R.S.R., and Zinolabedini, A.: Free Convection From a Vertical Plate With Nonuniform Surface Temperature and Embedded in a Porous Medium, *Transactions of ASME, Journal of Energy Resources Technology*, 109, 26–30 (1987).
- [8] Gorla, R.S.R., and Tornabene, R. Free Convection from a Vertical Plate With Nonuniform Surface Heat Flux and Embedded in a Porous Medium, *Transport in Porous Media Journal*, 3, 95–106 (1988).
- [9] Chen, H.T. and Chen, C.K.: Natural Convection of Non-Newtonian Fluids About a Horizontal Surface in a Porous Medium, *Transactions of ASME, Journal of Energy Resources Technology*, 109, 119–123 (1987).
- [10] Mehta, K.N. and Rao, K.N.: Buoyancy-induced Flow of Non-Newtonian Fluids in a Porous Medium Past a Horizontal Plate With Nonuniform Surface Heat Flux, *International Journal of Engineering Science*, 32, 297–302 (1994).
- [11] Nakayama, A. and Koyama, H.: Buoyancy-induced Flow of Non-Newtonian Fluids Over a Non-Isothermal Body of Arbitrary Shape in a Fluid-Saturated Porous Medium, *Applied Scientific Research*, 48, 55–70 (1991).
- [12] Nield, D.A. and Kuznetsov, A.V.: The Cheng-Minkowycz Problem for Mixed Convective Boundary Layer Flow in a Porous Medium Saturated by a Nanofluid, *International Journal of Heat and Mass Transfer*, 52, 5792–5795 (2009).
- [13] Nield, D.A. and Kuznetsov, A.V.: Thermal Instability in a Porous Medium Layer Saturated by a Nanofluid, *International Journal of Heat and Mass Transfer*, 52, 5796–5801 (2009).

- [14] Blottner, F.G.: Finite-Difference Methods of Solution of the Boundary-Layer Equations, *AIAA J.*, 8, 193–205 (1970).
- [15] Aldoss, T.K., Jerrah, M.A. and Duwari, H.M., Wall Effect on Mixed Convection From Horizontal Surfaces with a Variable Wall Heat Flux, *The Canadian Journal of Chemical Engineering*, 72, 35–42 (1994).
- [16] Lakshmi Narayana, P.A., Murthy, P.V.S.N. and Gorla, R.S.R.: Soret-driven Thermosolutal Convection Induced by Inclined Thermal and Solutal Gradients in a Shallow Horizontal Layer of a Porous Medium, *Journal of Fluid Mechanics*, 612, 1–19 (2008).